Adapting Taylor Dispersion to Microfluidics Scale

A Major Qualifying Project (MQP) Report
Submitted to the Faculty of
WORCESTER POLYTECHNIC INSTITUTE
in partial fulfillment of the requirements
for the Degree of Bachelor of Science in

Physics,
Mechanical Engineering

By:

Geneva Isaacson

Project Advisors:

Francesca Bernardi

Date: April 2021

Abstract

Microfluidics is a field that studies fluid mechanics phenomena within channels of length scales varying from micrometers to millimeters. Microfluidic applications span the fields of biochemistry, physics, materials science, chemical engineering, and microbial ecology. This Major Qualifying Project is focused on designing an experimental setup and protocol to observe the well-known theory of Taylor dispersion at the microscale. The ultimate goal of developing this experiment is to establish an accessible and repeatable way to determine the dispersion coefficient of solutes using microfluidics. The experiment consists in injecting fluorescein dye solution into a straight microchannel of rectangular cross-section with aspect ratio 0.25, and observe as it disperses downstream due to the interplay of advection and diffusion. A camera positioned $3\,cm$ away from the dye inlet hole, captures the solute evolution over time. Encouraging preliminary experimental results are able to reproduce Taylor dispersion at the microscale. The next steps will be to benchmark experimental results against known theoretically predicted dispersion coefficient values, and additional testing on microchannels with varying cross-sectional aspect ratios.

Acknowledgements

1. Professor Bernardi for advising me for a full year on this project. Professor Bernardi provided consistent support and advise throughout the extent of this project helping me to reach my goals.
2. Garam Lee for meeting with me to discuss past work that she had done on a similiar project. Her advise on injecting the dye bolus greatly supported the work done on this project.
3. Abigail Taylor for meeting with me to discuss benchmarking my experimental data with the theoretical data.
4. Spencer Francis for working in the lab with me. Even on separate projects, you provided support and knowledge as I learned about the lab.
5. LEAP for being a center that I was able to preform my experiments at.
6. Eli Silver for providing my project with 3D printed gaskets to ease the experimental set up.
7. Jim Eakin
8. Professor Petkie
9. Jake Bouchard

Contents

List of Tables

List of Figures

1 Introduction

Microfluidics is an interdisciplinary field of science and engineering that studies the behavior, control, and manipulation of fluids in channels with dimensions on the order of micrometers. The small scale of microfluidic systems enables researchers to investigate fluid dynamics and transport phenomena with high precision and accuracy, making them particularly useful for applications in biotechnology, chemistry, and materials science.

A classic phenomenon in fluid mechanics, known as "Taylor dispersion," refers to the boost in spreading of a passive solute in laminar shear flow due to the interplay between molecular diffusion and advection. Taylor dispersion is named after the British mathematician and physicist G.I. Taylor, who first described the phenomenon in the early 1950s [1]. The understanding of Taylor dispersion is crucial in many applications, such as mixing and de-mixing of solutes, calculating dispersion coefficients and absorption rates, and determining optimal velocities and flow rates for fluids [2, 3].

This Major Qualifying Project has the immediate goal of developing a repeatable and accessible procedure to observe Taylor dispersion at a microfluidics scale. This requires adapting the experimental setup developed by Taylor in three-dimensional large-scale cylindrical pipes to microfluidic-scale rectangular channels. The ultimate goal of developing such experimental setup and protocol, is to employ it as a way to consistently and accessibly measure solute dispersion coefficients.

Four main tasks are required to execute the project and will be covered by this report: fabrications of microchannels, design of the experimental setup, experimental protocol development, and data analysis. The next steps of this project would focus on the benchmarking of the experimentally computed dispersion coefficient of fluorescein against theoretical predictions. Ultimately, this project is a jumping off point to develop a robust experimental procedure to measure the dispersion coefficient of solutes that must be valid for microchannel domains of all aspect ratios.

2 Background

This project has the ultimate goal of developing a repeatable and accessible experimental procedure to consistently measure solute dispersion coefficients at the microscale leveraging the phenomenon of Taylor dispersion. The first step to achieve such an ambitious goal is to design and implement an experimental setup and protocol that allow to observe Taylor dispersion at the microscale. Therefore, we consider microchannels with rectangular cross-sections where a is the half-height of the channel and b is the half-width of the channel, as shown in Figure 1.

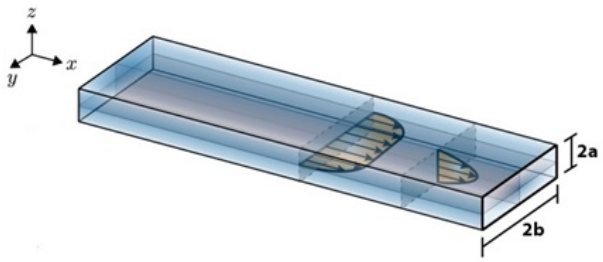

Figure 1: Diagram of 3D microchannel with rectangular cross-section, $2a \times 2b$. Here, a is the half-height of the channel and b is the half-width of the channel. Figure adapted from [4].

2.1 Taylor dispersion

Taylor dispersion is a phenomenon observed when passive solutes simultaneously undergo laminar advection and diffusion in a straight pipe. Advection and diffusion are two fundamental mechanisms that govern fluid and particle transport in fluid mechanics and microfluidics. Advection describes the transport of substances due to the bulk motion of a fluid. Diffusion describes the molecular motion of fluid particles typically from a region of higher concentration to a region of lower concentration. The advection-diffusion equation describes the transport and molecular diffusion of a substance in a fluid flow; it is a key equation in fluid mechanics and is widely used to model the transport of solutes in laminar flows.

While G.I. Taylor's result from the 1950s [1] is for three-dimensional (3D) macroscopic circular pipes, this project focuses on 3D microscopic microchannels with rectangular cross-sections, as shown in Figure 1. Though the channels used in this report are 3D, the camera view for the experiment is top-down, effectively showing an xy-cross-section of the microchannel and flattening the geometry z-direction. As such,

we model the physics of the problem in 2D and report the corresponding advection-diffusion equation:

$$\frac{\partial C}{\partial t} + u \cdot \nabla C = \kappa \nabla^2 C, \tag{1}$$

where C is the concentration [g/L] of the solute being transported and diffusing, t is time [seconds], and κ is the solute molecular diffusivity $[m^2/s]$. Here, $u = u(y)$ is the laminar steady-state solution to the Naiver-Stokes equations with no-slip boundary conditions (no flow at the walls) driven by a negative pressure gradient:

$$\frac{d^2u}{dy^2} = \frac{2\,p_x}{\mu}, \qquad\qquad u(y = \pm b) = 0, \tag{2}$$

where $\nabla p = p_x < 0$, the factor of 2 is for convenience, y is the transverse distance from the center of the channel cross-section (see axis on Figure 1), μ is the dynamic viscosity of the fluid $[kg/(m\,s)]$, and b is the half-width of the channel. This leads to a parabolic flow profile for $u = u(y)$:

$$u = U\left(1 - \frac{y^2}{b^2}\right), \tag{3}$$

where U is the centerline maximum velocity in the channel [1]. Equation (3) is the flow velocity driving the advection term $(u \cdot \nabla C)$ in equation (1).

Taylor dispersion describes the boost in diffusivity of a passive solute in laminar shear flow due to the interplay of molecular diffusion and advection. A tracer is considered passive if it does not chemically interact with the surrounding fluid when injected into a fluid flow [5]. Taylor dispersion affects solutes being transported in laminar flow, when fluid particles move in smooth, parallel layers or streams, with little or no mixing between the layers. For laminar flow, particles move in an orderly manner, without turbulence or chaotic movement [1]. This type of flow, shown at the top of Figure 2, is characterized by a low Reynolds number; the Reynolds number is a dimensionless parameter that describes the relative importance of inertial to viscous forces in a fluid. It is utilized to categorize fluid systems by how important viscosity is in controlling the flow of the fluid, and is defined as:

$$Re = \frac{\rho\,U\,L}{\mu}, \tag{4}$$

where ρ is the density of the fluid $[g/m^3]$, U is the characteristic flow speed $[m/s]$, L is the characteristic length $[m]$, and μ is the dynamic viscosity of the fluid $[kg/(m\,s)]$. Due to the geometry of our experimental channel, we define the characteristic length in terms of the microchannel cross-sectional dimensions as $L =$

$4ab/(2a + 2b)$, which provides an updated version of the Reynolds number formula:

$$Re = \frac{4ab\,\rho\,U}{(2a + 2b)\mu}, \tag{5}$$

where, again, a and b are the half-height and the half-width of the channel in m, respectively. At Reynolds number values greater than 3500, when inertia dominates over viscous effects, fluid flows are considered turbulent with significant mixing between the layers, as shown in the bottom of Figure 2. A Reynolds number much less than 1 indicates viscous flow [6]. For the scope of this experiment, the Reynolds numbers are low, $Re \sim 1$. Due to the very small length-scales in microfluidic settings, here a low Reynolds number can be achieved for non-viscous fluids (like deionized water).

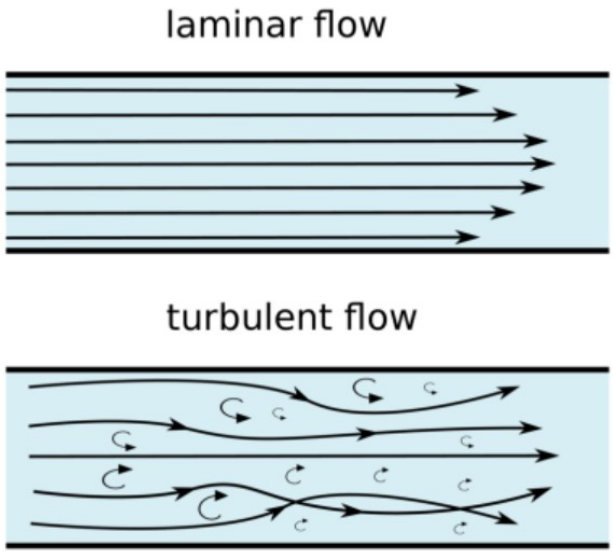

Figure 2: Laminar flow (top) is characterized by orderly movement of particles. Turbulent flow (bottom) involves chaotic movement, mixing, and turbulence. The Reynolds number for our experiments is of order 1, placing it in the laminar flow regime. Figure from [7].

Figure 3 shows the time and space evolution of a passive tracer injected into laminar shear flow in a straight channel as it is transported downstream and undergoes Taylor dispersion. There four different stages can be described as follows, top to bottom. When the solute is introduced into the microchannel in the first row of Figure 3, it is uniform across the cross-section. In the intermediate time steps shown as the second and third rows in Figure 3, the dye is initially transported by the background flow and takes a parabolic flow profile. Here, the dye at the center of the channel moves more quickly than the dye at the channel walls due to the no-slip condition. At the same time, molecular diffusion acts on the solute and drives the back particles inward and the front particles towards the channel walls distorting the parabolic profile. Finally, as shown in the fourth row of Figure 3, at long-time and as it reaches downstream, the dye

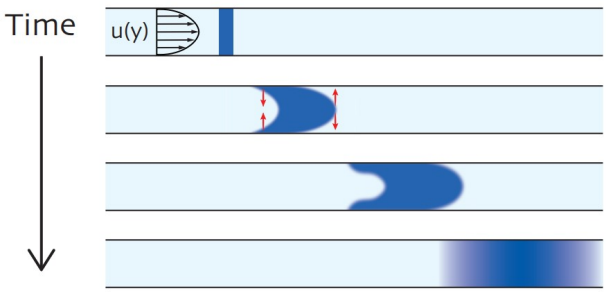

Figure 3: Space and time evolution of a passive tracer (blue) injected into laminar parabolic shear flow in a straight channel. First row: An initial plug of dye uniform across the cross-section is injected in 2D parabolic laminar flow. Second row: At intermediate times, the solute is being transported downstream and takes a parabolic profile. At the same time, molecular diffusion pushes solute particles inward and outward (red arrows) at the dye tails and front, respectively. Third row: As times passes, molecular diffusion acts with transport to blur and distort the parabolic profile, push the back particles towards the centerline and the front particles towards the walls of the channel. Fourth row: At long-time the solute is uniformly dispersed along the channel's cross-section and longitudinally displays a Gaussian profile. Figure adapted from [4].

concentration returns to be uniform across the cross-section as it widens in the longitudinal direction with a Gaussian profile. This happens at times long past the diffusion timescale, defined as $t_d = a^2/\kappa$ [1].

For rectangular microchannels, dispersion reaches 95% of its asymptotic value after a wait-time t_w (in seconds) has passed:

$$t_w = \frac{1}{5}\frac{b^2}{\kappa}. \tag{6}$$

In our experiment, we will wait longer than t_w to ensure the solute is dispersed past transitional times before activating the background flow to create an initial condition that mimics the one shown in the first row of Figure 3 [3, 4]. As the solute is transported through the channel, its particles experience random motion due to molecular diffusion, which causes it to spread out over time. Its dispersion is influenced by factors such as the diffusion coefficient κ, the channel aspect ratio a/b, and the Péclet number. The Péclet number is a nondimensional parameter describing the relative importance of advection and diffusion; it is defined as:

$$Pe = \frac{Ua}{\kappa}. \tag{7}$$

At low Péclet number values, diffusion is the dominant effect, while at high Péclet numbers, advection dominates over diffusion. In Taylor dispersion, the Péclet number is large due to the shear-induced dispersion which is predominantly due to advection. But this does not mean that diffusion has no influence on the solute: as established, Taylor dispersion describes the boost in diffusivity due to the interplay of the two

effects. That is, the enhanced dispersion coefficient K $[m^2/s]$ is given by:

$$K = \kappa + \frac{2}{105}\frac{a^2U^2}{\kappa}f, \tag{8}$$

where a, U, and κ are defined as above, and f is a computable factor which depends on the channel cross-sectional geometry [1, 3, 8]. This is an enhanced diffusivity compared to simple molecular diffusion because of the additional term that is inversely proportional to κ; typically, the value of κ is small, generating $K \gg \kappa$.

When enough time has passed and the solute is in the Taylor dispersion regime, its concentration distribution is well-described by a Gaussian function:

$$C(x,t) = \frac{C_0}{\sqrt{4\pi Kt}}\, e^{-(x-Ut)^2/4Kt}, \tag{9}$$

where C_0 is the initial concentration, K is the enhanced dispersion coefficient defined in (8), t is time, x is the position along the axial direction, and U is the flow rate [9]. The enhanced dispersion coefficient can be written in terms of the Péclet number and the dispersion factor f $[s/m^2]$, as done in [3]:

$$\frac{K}{\kappa} = 1 + \frac{2}{105}\left(\frac{Ua}{\kappa}\right)^2 f = 1 + \frac{2}{105}\,Pe^2\, f. \tag{10}$$

The expression for the enhanced dispersivity defined in equation (10), can be computed using known dispersion factor, fluid properties, and channel dimensions. The ultimate goal of this project is develop an experimental setup and protocol to reliably measure the K and f values which match predicted values for known geometries.

2.2 Accessible microfluidic experiments

There are many benefits that come from downsizing standard laboratory procedures to the field of microfluidics, such as, minimizing the cost, space, and materials needed to run experiments which may lead to an increase in productivity for applications [9]. However, despite the smaller scale, most microfluidics fabrication techniques are neither easily accessible or affordable.

The two most common traditional manufacturing techniques for microfluidic channels are photolithography and soft lithography. Photolithography is a procedure that uses light to transfer a pattern onto a substrate. It involves coating a substrate with a photoresist, exposing it to light through a photomask, and then developing it to reveal the pattern [10]. Photolithography requires costly equipment such

as a photomask aligner and exposure system, making it a relatively expensive technique [10]. The lowest possible cost for the production of one microchannel using photolithography is approximately $6,000 [11].

Soft lithography is also a widely used technique for fabrication of microfluidic devices. It uses a patterned elastomeric stamp made of polydimethylsiloxane (PDMS) to transfer a pattern onto a substrate. The process involves several steps, including mold fabrication, PDMS replica casting, and bonding to a substrate [10]. Currently, the cheapest procedure to fabricate microchannels using soft lithography costs around $10,000 [11].

Other techniques, although less common, consist of injection molding, 3D-printing, and laser ablation; these can also be quite expensive and less than accessible. We at the Fluid Mechanics and Small-Scale Transport Lab (FMNST Lab) at Worcester Polytechnic Institute employ a manufacturing technique involving a commercially available craft cutter, polyimide tape, and acetate sheets, to produce microchannels in house for approximately $350. This repid-prototyping technique was initially developed at the Harris Lab at Brown University in 2019 to generate microchannels in an accessible, inexpensive way [4].

3 Methodology

The experimental procedure for this project consists of three phases: microchannel fabrication, experimental run, and data processing. A complete list of materials for fabrication and experimental equipment is reported in Appendix A.

3.1 Microchannel Fabrication

In the past, microchannel fabrication has imposed a cost barrier to perform microfluidics experiments. In this project, an accessible way to rapidly fabricate microchannels first introduced by Taylor and Harris [9] and extended by Lee *et al.* in 2019 [12] was further studied. Using a commercially available Silhouette Cameo 4 craft cutter, microchannels can be manufactured precisely with smooth walls and at a low cost.

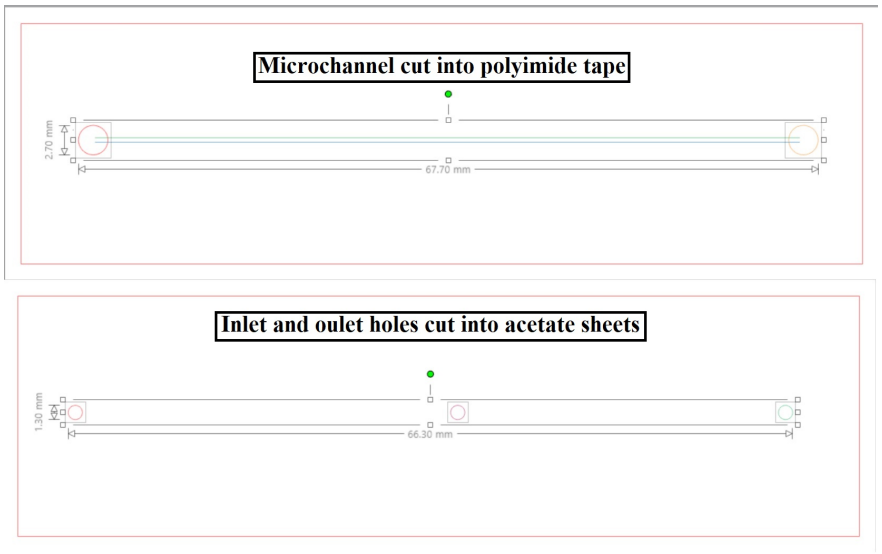

Figure 4: Snapshot of Silhouette Studio Design software programmed to cut polyimide tape microchannels (top) and acetate sheet inlet and outlet holes (bottom).

The first step in the fabrication process consists in programming the freely downloadable "Silhouette Studio Design" software [13] to cut microchannels of the desired shape. The software allows for dimensions as small as 250 micrometers with smaller designs needing to be imported from an external program [4]. For all microchannels constructed, polyimide tape (Bertech, $1\,in \times 36\,yd$) and acetate sheets (Clear DuraLar Polyester Film, $0.004\,in/100\,\mu m$ thickness) are put through the craft cutter. The polyimide tape is used to cut the microchannel so it forms its walls, while the acetate sheets are used to seal the microchannel above and below. The microchannel design programmed in the Silhouette Studio software has a straight

rectangular shaped channel with circular openings at both ends which will serve as solute inlet and outlet, as shown at the top of Figure 4. The bottom half of Figure 4 shows the cuts to be made into the acetate sheet that produce inlet and outlet holes for fluids to enter and exit the channel. Note that there is a dye inlet hole $2.5\,cm$ away from the deionized (DI) water inlet. From the dimensions in Figure 4, it can be seen that the inlet and outlet holes on the acetate sheet are smaller than the microchannel cavities to allow for easier filling of the microchannel and to ensure that there is enough space for the fluids to enter and exit. The software displays the designs as they will be seen when they are cut by the craft cutter.

We fabricate channels following the rapid prototyping techniques described in [4, 9, 12]. For a full step by step fabrication protocol please see Appendix C. However, we introduce a new 3D-printed gasket in the experimental setup to connect injection tubing to our microchannels; this is based on a design by Eli Silver from the Harris Lab at Brown University. The tubing allows for solute injection through a Harvard Apparatus Standard Infuse-Withdraw Pump 11 Elite. Around the inlet hole of the microchannel, we place a small disk of polyimide tape with an inner radius matching that of the inlet hole; this step is shown in Figure 11. Then, we screw the 27 gauge plastic tip of a syringe (Stainless steel dispensing needle with luer lock connection, $1/2\,in$, 27 gauge) onto the gasket, and align it with the inlet hole around which we have placed the polyimide ring. We attach the gasket to to the microchannel superglue (Starbond EM-150 medium instant premium CA superglue) with a quick dry hardener spray (Starbond CA glue accelerator). Under a fume hood, using a precision tip, glue is used to seal the gasket onto the top acetate sheet of the microchannel. The glue is sucked under the gasket due to capillary action. Then, the setup is sprayed with the glue accelerator and left to dry in the fume hood for 20 minutes, completing the fabrication of the microchannel. The last step of the process is to remove the syringe tip used to line up the gasket and the inlet hole, and the microchannel is ready to be used for testing.

3.2 Calibration Test

To visualize and track solute dispersion in the microchannel, $0.55\,g/L$ of fluorescein sodium salt are mixed in DI water to form a passively spreading solution [14]. The concentration of fluorescein used for the experiment is selected based on the results from the calibration test discussed in this section. Fluorescein salt has a molecular diffusion coefficient of $\kappa = 5.7 \times 10^{-6}\ cm^2/s$ [9]. We use fluorescein dye in order to track dispersion using a camera and the fluorescein concentration used to mix the dye solution is chosen based on dispersivity, camera settings, and the lighting of the system. The camera measures pixel light intensity (in the RGB channels), yet we can only control the concentration of the dye when mixing the solute. Therefore, we carry out a calibration test to find where there is a linear relationship between dye

intensity and concentration; this allows us to mix dye solutions at concentrations in the correct regime, so that concentration can be used as a proxy for intensity in our data analysis.

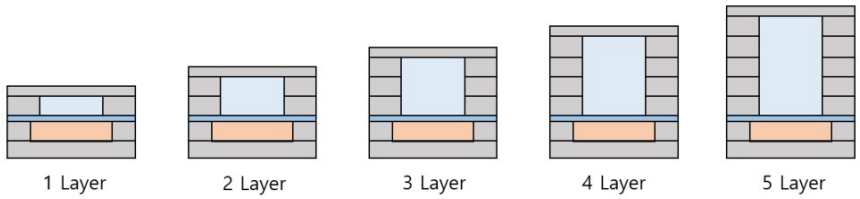

Figure 5: Microchannels of increasing thickness for intensity calibration test. Number of tape layers used to build microchannels of various thickness increases left to right, with the leftmost channel being $106.5\,\mu m$ and the rightmost channel being $532.5\,\mu m$ thick. Figure from [12].

For the calibration test, channels are fabricated using the techniques described in Section 3.1, yet are stuck together before adding a final layer of acetate to generate channels of increasing thickness using 1 to 5 layers of tape, as shown in Figure 5. To find the linear regime between dye intensity and concentration, 5 different concentrations of dye are mixed in DI water and are each tested on five microchannels, ranging from 1 to 5 layers of thickness; Figure 6 shows the 25 channels we build and fill with five dye solutions. The first column is filled with $0\,g/L$ concentration of fluorescein dye (i.e., pure DI water), the second column is filled with $0.1\,g/L$ concentration of fluorescein dye, the third column with $0.3\,g/L$ concentration, the forth column with $1\,g/L$ concentration, and the fifth column with $3\,g/L$ concentration of fluorescein dye. Each row in Figure 6 includes microchannels of the same thickness, with the first row including microchannels built using one layer of polyimide tape all the way to the fifth row which includes microchannels built with five layers of polyimide tape stuck together. The linear regime is identified by taking images of all twenty-five microchannels and plotting their intensity of dye versus a product of the number of layers with the concentration of dye.

Photos of each of the microchannels are taken using a Nikon D500 camera with a macro lens (Mitakon Zhongyi $20\,mm$ f/2 super macro). The camera is set to manual mode with a shutter speed of $1/100\ s$ and ISO 800. The "Image Quality" is set to 'JPEG Fine' and the "Image Size" is set to 'Large.' The macro lens is set to be in a fully open aperture position of F2 with $\times 4.0$ magnification. A tripod is used to position the camera facing top down onto the microchannels as shown in Figure 9. Underneath the experimental setup is a light panel (Kaiser slimlite plano 5000 K lightbox $16.9\,in \times 12.2\,in$) which helps to back-illuminate the channels. Attached to the top of the Nikon D500 digital camera, there is a flash (On-camera LED-36x video light with a pack of four AAA batteries) which helps to brighten up photos for better intensity readings.

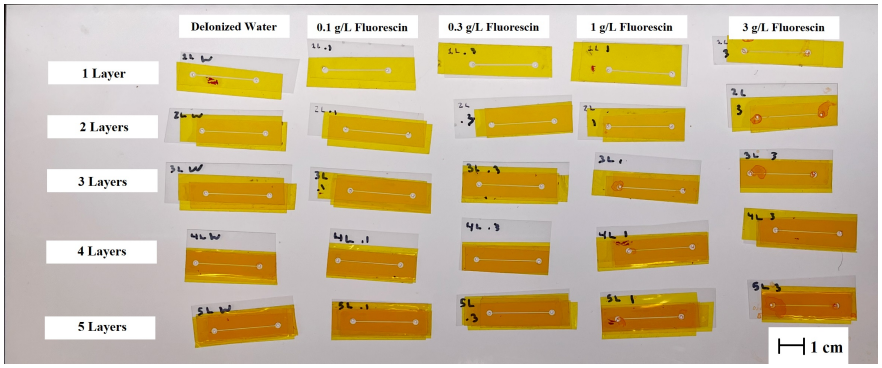

Figure 6: Microchannels for intensity calibration. Each row includes channels of the same thickness, with the first row aligning channels made from one layer and the fifth row containing channels made of five layers of polyimide tape stuck together. Microchannels along each column are filled with the same fluorescein dye solution, with concentrations increasing left to right starting with DI water ($0\,g/L$) and ending with $3\,g/L$.

Twenty-five photos are taken (one for each of the microchannels in Figure 6) and edited down to be 1500×150 pixels. Then, images are run through a Matlab code (included in Appendix B) which crops the same channel section from each photo and outputs its mean, minimum, and maximum intensity values (plotted in Figure 7).

A different visualization of the same data is shown in Figure 8. Here, for each intensity output the number of layers is multiplied by the concentration of fluorescein solute in each microchannel. Figure 8 shows all data points in order which allows us to identify a linear regime between intensity and concentration. We find a linear fit for the first 16 data points which allows us to select concentrations that produce intensity values below maximum threshold of 255 readable by the camera. As long as the values of intensity are below 255, the linear regime for this calibration test can be quantified by:

$$\text{Intensity} = 121.28\,(\text{Thickness [\# of layers]})\,(\text{Concentration [g/L]}) + 50.54. \tag{11}$$

Hence, we choose a $0.55\,g/L$ dye concentration to produce our experimental fluorescein solution to guarantee that our solute falls within the linear regime remaining well below the 255 threshold.

3.3 Experimental Testing

The experimental setup is shown in Figure 9. The microchannel is supplied a working fluid of deionized water through a syringe pump (Harvard Apparatus Standard Infuse-Withdraw Pump 11 Elite). The working fluid is in a glass syringe ($500\,\mu L$, Model $750L$) with a plastic syringe tip (27 gauge, point style 3) connected to capillary tubing (Cole Parer PTFE #30 AWG thin wall tubing). The capillary tubing is attached to a

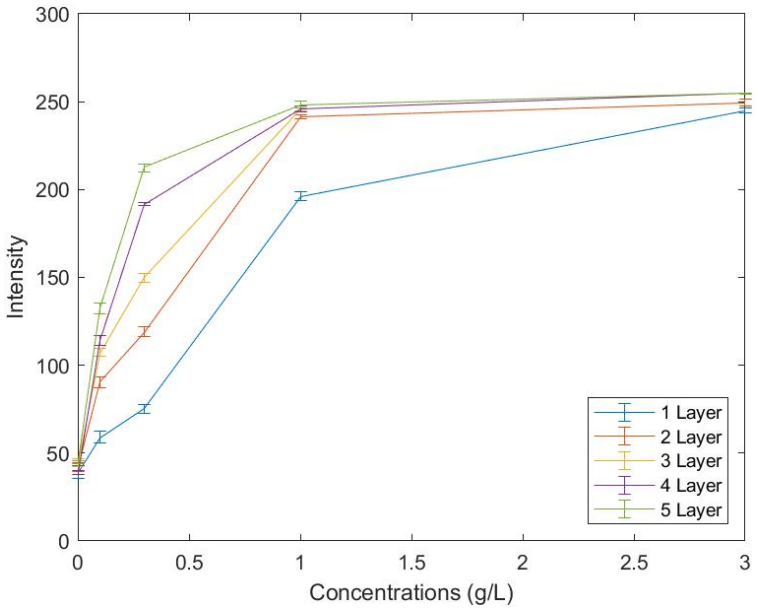

Figure 7: Intensity calibration test showing dye intensity *vs.* concentration. Five images were taken (one for each channel thickness) for each dye concentration. The mean intensity value for each image is shown aligned vertically at fixed concentrations $0\,g/L$, $0.1\,g/L$, $0.3\,g/L$, $1\,g/L$, and $3\,g/L$. The , minimum and maximum values are shown using error bars. Each color represents a different channel thickness, with thickness increasing bottom (one layer channels, blue) to top (five layer channels, green).

27 gauge blunt tip which is then screwed onto the gasket for the working fluid to enter the microchannel at a constant flow rate. Underneath the microchannel is a light panel (Kaiser slimlite plano 5000 K lightbox $16.9\,in \times 12.2\,in$) which illuminates the channel from below. Above the microchannel there is a Nikon D500 camera that captures photos of the channel top down mounted with a marco lens (Mitakon Zhongyi $20\,mm$ f/2 super macro). The camera is held up with a tripod (Vanguard alta pro 263AP aluminum-alloy tripod) so that is can be kept in the same position for all experiments. Attached to the top of the camera, there is a standard flash (On-camera LED-36x video light with a pack of four AAA batteries). This allows for more lighting on the microchannel. The camera is activated remotely using a programmable trigger (Wireless shutter TW-283 DC0/DC2) which allows for photos to be taken at a consistent rate of 1 frame per second for the entirety of the experimental run. The resolution of the images taken in this setup is 9.92756×10^5 pixels per meter.

Figure 10 shows three syringe tips on the left and three syringes on the right. The two plastic syringes (first and second from the left) have a rubber seal which produces friction between the barrel and the plunger. Because of this, using a glass syringe (shown at the far right of Figure 10) in the syringe pump is required for these microfluidic experiments. Glass syringes have a small gap between the plunger and the pusher block which allows the syringe to move with negligible friction [12]. To further allow for the syringe

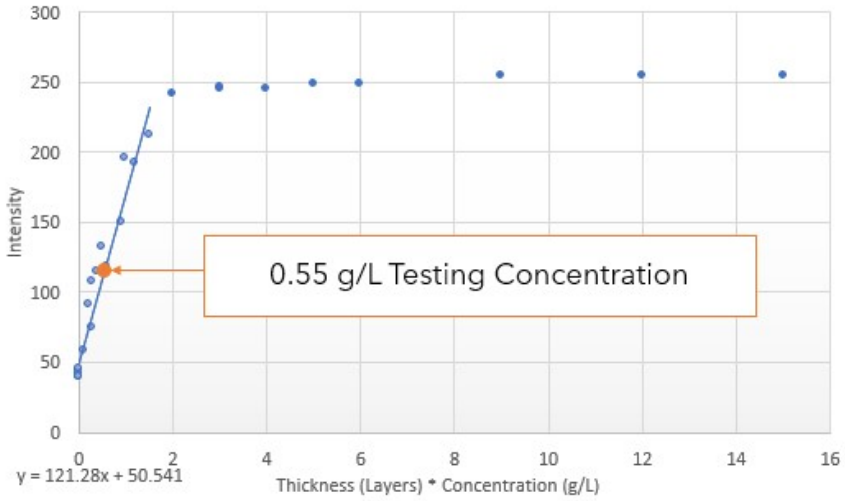

Figure 8: Dye calibration results plot showing intensity *vs.* (concentration)(thickness). The horizontal axis represents the concentration (in g/L) times the thickness (in number of tape layers) of the point and the vertical axis represents the intensity output from Matlab. The linear fit of $y = 121.28x + 50.541$ is for the first 16 data points as these are the ones that are all well under intensity 255, which is the maximum camera threshold. The selected dye concentration of $0.55\,g/L$ is shown in orange.

to have the least amount of external forces, a smaller inner diameter is desired [12]. Because of this, we use a Hamilton 500 glass syringe in the syringe pump with an inner diameter of $6.6\,mm$. This Hamilton 500 glass syringe is mounted with a 27 gauge $2\,in$ plastic tip (last syringe and last tip on the right of Figure 10, respectively) and has a volume of $0.5\,mL$; this is more than enough for a full experimental run. We use the 27 gauge plastic tip (Figure 10, left) with the $1\,mL$ plastic syringe (Figure 10, center) to insert dye into the dye inlet hole, and the 30 gauge plastic tip (Figure 10, center) with the $3\,mL$ plastic syringe (Figure 10, left) to fill the glass syringe with DI water.

One of the key concerns when running experiments is to ensure that there are no air bubbles within the tubing, syringe tip, and glass syringe. When air bubbles form, there is no way to ensure that the flow rate in the channel is controlled at the rate set on the syringe pump. Bubbles in the tube can also get pushed into the microchannel causing a section of the channel to have no fluid in it [12]. In order to avoid bubbles when filling the channel, we fill it at the very slow flow rate of $1\ \mu L/min$. Also, we check to make sure that there are no bubbles within the syringe or the tip which helps to ensure that no bubbles form in the tubing. Once the absence of bubbles within the system is confirmed, we can proceed with experimental testing.

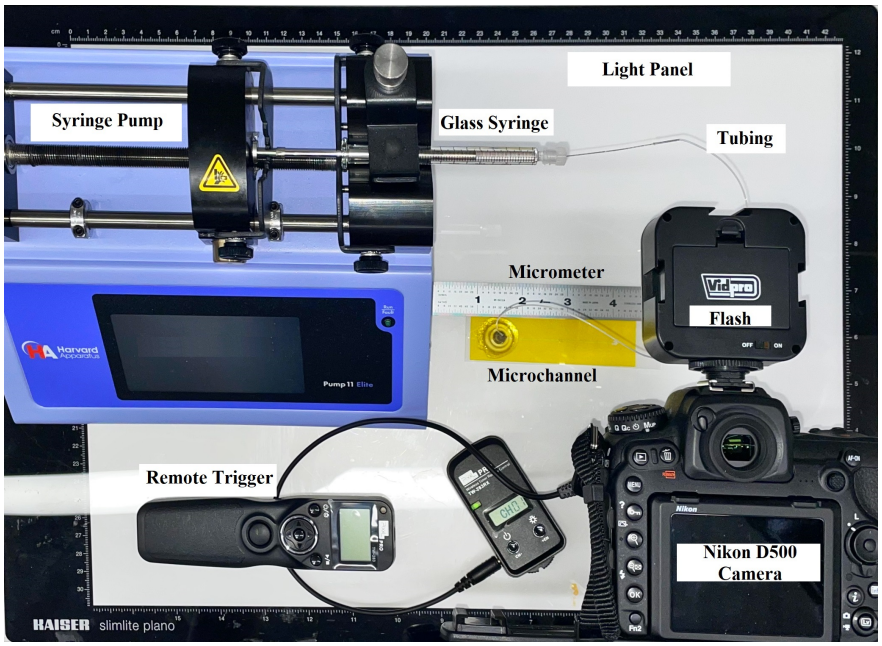

Figure 9: Photo of the experimental setup which contains from top to bottom, left to right: syringe pump, remote trigger, glass syringe, micrometer, microchannel, light panel, tubing, flash, and Nikon D500 camera. For a full list of equipment used, please see Appendix A.

3.3.1 Experimental Run

Once it is confirmed that there are no bubbles in the system, the desired flow rate is programmed into the syringe pump. The syringe pump is turned on at a flow rate of $2.4\,\mu L/min$ until there is excessive water coming out of the microchannel outlet hole to avoid hydrostatic pressure. Once there is sufficient water exiting the channel, the syringe pump is stopped, and the excess water is wiped away.

After waiting for at least 1 minute for the stabilization of the system, the dye inlet hole is uncovered. Using the edge of a Kim wipe, a small amount of DI water is removed from the channel. Then, using a $1\,mL$ plastic syringe with a 30 gauge tip, a tiny droplet of fluorescein dye solution is placed into the dye inlet hole and the hole is sealed using a small piece of polyimide tape. The polyimide tape covering is constructed using two pieces of circular tape. The larger piece of tape has a diameter of $4\,mm$. The small piece of tape has a diameter of $1.3\,mm$, which is the same size as the dye inlet hole. The smaller piece of tape is placed at the center of the larger one. This covering is then perfectly lined up with the dye inlet hole and placed down, creating a perfect seal in the dye inlet hole as shown in Figure 11. As mentioned, for this experiment the dye inlet hole has a diameter of $1.3\,mm$ but in general, it should never be larger than $2\,mm$ [12]. Appendix D reports the procedure to manufacture the dye inlet hole covering. Once the dye inlet hole is covered, we wait for the required wait time, t_w, defined in Equation (6) to pass to ensure that the dye is fully diffused

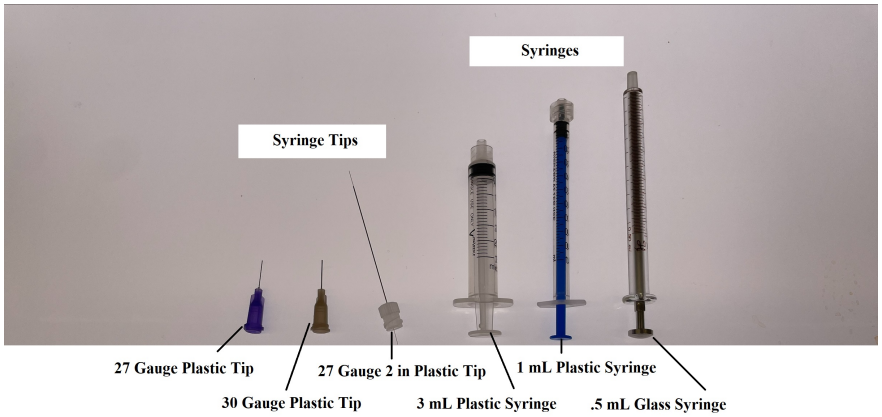

Figure 10: Different types of syringe tips and syringes. Shown left to right: 27 gauge plastic tip, 30 gauge plastic tip, 27 gauge 2 inch plastic tip, 3 mL plastic syringe, 1 mL plastic syringe, and 0.5 mL glass syringe. In our experiment, we use the 27 gauge plastic tip with the 1 mL plastic syringe to insert dye into the dye inlet hole. We use the 30 gauge plastic tip with the 3 mL plastic syringe for filling the glass syringe with DI water. We use the 27 gauge 2 inch tip and the 0.5 mL glass syringe for injecting DI water into the channel with the syringe pump.

across the channel width before starting the syringe pump. Hence, the syringe pump is programmed to run at a flow rate of $2.4\,\mu L/min$ and turned on in the 'Infuse Rate' mode. Simultaneously, the remote trigger is activated to capture photos every 1 second for 5 minutes. Using the timer option, the remote can be set to take a set number of photos at a set speed.

3.4 Data Analysis

The experimental data collection consists in dye intensity values recorded through imaging. The camera is placed $3\,cm$ downstream from the dye inlet hole to observe changes in intensity over time through the course of an experiment. All experimental photos are run through a Matlab script (available in Appendix E) which performs the following tasks:

1. All experimental images are uploaded into Matlab in the order at which they were captured during the experiment.

2. Due to the similarity of the bright yellow-orange color of the fluorescein dye solution and the polyimide tape, the blue channel is isolated from the RGB and inverted. This converts the photo into a black and white scale where black shows a zero intensity and white shows the maximum intensity readable by the camera of 255.

3. The channel is rotated to be horizontal. This is done by having the user select four points from a

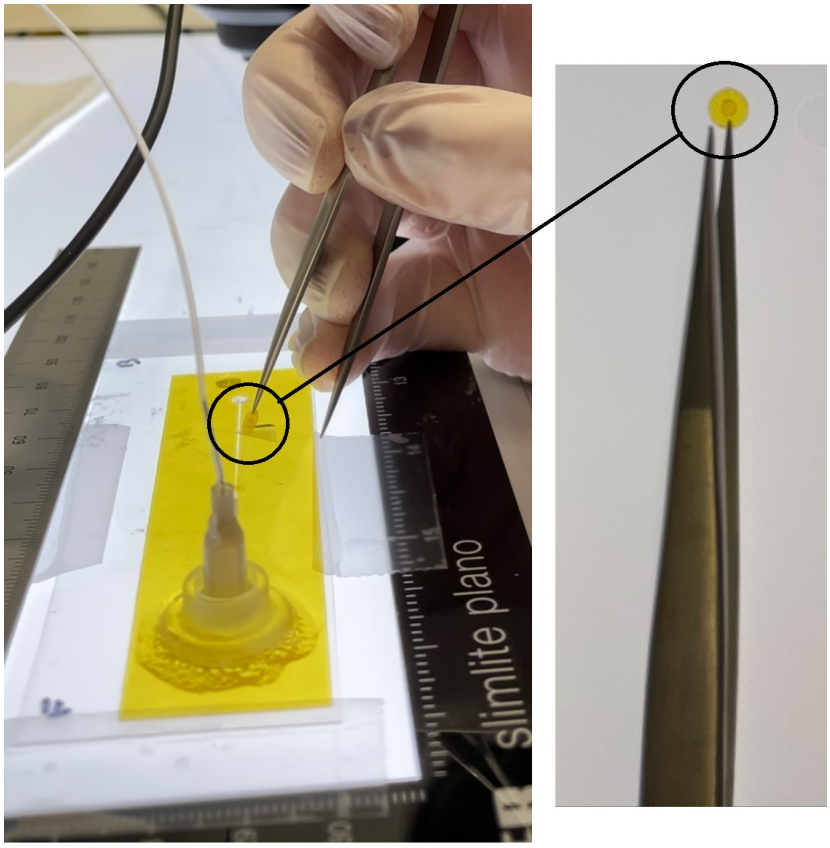

Figure 11: The dye inlet hole cover is built from two concentric circles of polyimide tape. The smaller circle with a diameter of $1.3\,mm$ is stacked on the larger circle with a diameter of $4\,mm$; the smaller circle has the same size as the dye inlet hole so it can be used to perfectly seal it once a tiny dye droplet has been introduced in the microchannel.

reference image: two on the top channel wall, one on the left and one on the right, and two on the bottom channel wall, one on the left and one on the right. This allows Matlab to compute the slope of the walls and using trigonometry, the channel is rotated to become completely horizontal.

4. A section of the channel is cropped. Using a box selection in Matlab, the user crops a large region of the channel in the center from which the data will be acquired. The cropped region should be as close to the boundaries of the channel as possible without cutting into the polyimide tape.

5. The intensity of the dye from the cropped region is averaged in the x- and y-direction, resulting in a single averaged intensity value for each of the photos.

6. The last step is to plot the averaged intensity versus time for each experiment, as done in Figure 12 for two experiments.

4 Results

Experimental trials are completed for microchannels with a cross-sectional aspect ratio of $a/b = 1/4$. The dye bolus is placed into the microchannel and is transported downstream at a constant flow rate of $0.001\,m/s$ which corresponds to a volumetric flow rate of infusion of $2.4\,\mu L$ on the syringe pump. The Reynolds number for this experiment is $\mathrm{Re} \sim 0.06$ while the Péclet number is $\mathrm{Pe} \sim 88$.

We compute the entrance length, l_e, as the distance the DI water flow needs to cover before becoming fully developed; this will determine how far from the DI inlet we need to place the dye inlet hole:

$$l_e = 0.05 \left(\frac{4 \cdot 2a \cdot 2b}{4(a+b)} \right) Re. \tag{12}$$

Based on our experimental parameters, the entrance length of the flow condition is $0.4\,\mu m$ from the laminar flow inlet; this means that the dye inlet hole must be located at a distance greater than $0.4\,\mu m$ from the DI inlet. We position it $2.5\,cm$ away in orer to make it easier to insert dye.

With a microchannel cross-sectional domain of $a = 50.5 \times 10^{-6}\,m$ and $b = 200 \times 10^{-6}\,m$, the diffusion timescale is computed to be $t_d = a^2/\kappa \sim 4.5\,s$. For rectangular channels, the dispersivity reaches 95% of its asymptotic value on the timescale t_w, reported in equation (8), so we wait $14.5\,s$ for the dye bolus to diffuse without background flow before starting the syringe pump. This means that the camera must be placed at least $1.4\,cm$ downstream from the dye inlet hole to ensure that there is enough time for the solute to fully disperse. Hence, images are taken $3\,cm$ away from the dye inlet hole in order to record the phenomenon of Taylor dispersion. Here, we expect the solute concentration to have a Gaussian-like profile which in the long-term will allow us to compute the dispersion coefficient K_{exp} and dispersion factor f_{exp} from equation (10) and compare them to known theoretical values. Experimental parameters are reported in Table 1.

Variable	Units	Value	Definition
a	50.5×10^{-6}	m	Channel half-height
b	200×10^{-6}	m	Channel half-width
U	0.001	m/s	Fluid velocity
C	0.55	g/L	Solute concentration
Q	2.4	$\mu L/min$	Volumetric flow rate (syringe pump)
x_c	0.03	m	Camera location (from dye inlet hole)
κ	5.7×10^{-10}	m^2/s	Molecular diffusivity of solute
t_w	~ 14.5	s	Dispersion wait-time for initial condition

Table 1: Experimental parameters: symbols, values, units, and descriptions.

We generate plots showing dye solution intensity versus time based on a sequence of 300 photos taken every second for 5 minutes at a fixed camera location, as discussed above. We take photos of the dye flowing through a fixed cross-sectional slice of the channel of width $2b$ in the transverse direction and length 250 pixels in the axial direction. As time goes on, the solute flows through the camera frame which allows for the trailing edge of the solute more time to diffuse. Therefore, we expect the concentration profile to be asymmetrical. Figure 12 shows results from two experimental runs with the parameters reported in Table 1.

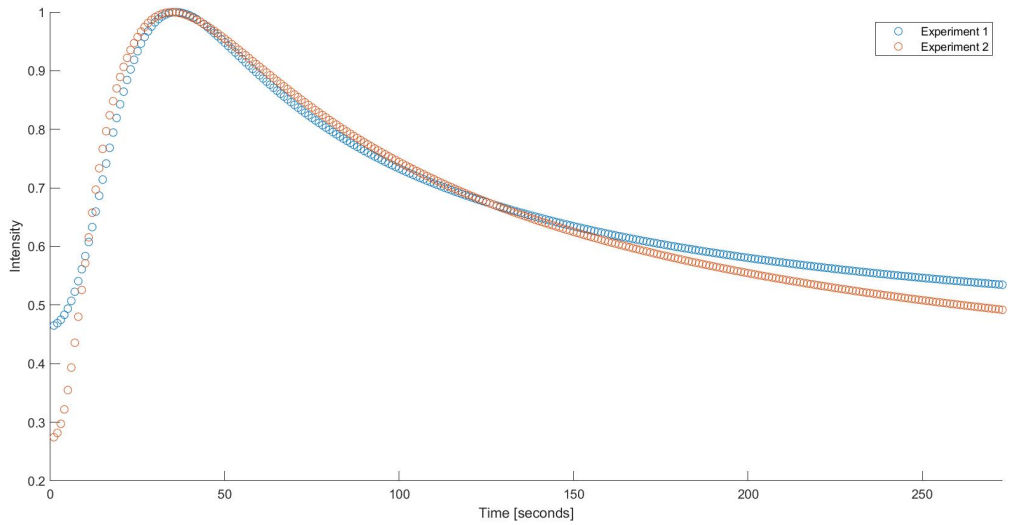

Figure 12: Scatter plot of data from two experimental runs superimposed. The curves show how the dye intensity in a cropped region of domain $2b \times 250$ pixels changes over time.

Figure 13 reports the averaged experimental data from the two runs shown separately in Figure 12. The green shading represents one standard deviation in each direction. Due to the variation in the initial conditions, both data sets have been normalized to peak 1; we achieve this by identifying the maximum intensity value reached by each experiment and dividing the corresponding data set images by its value. The slim standard deviation provides encouraging evidence that the experimental setup and protocol implemented in this project are able to produce repeatable results.

5 Conclusion

In summary, in this project we have been able to successfully manufacture microchannels utilizing a Silhouette Cameo craft cutter and use them to reproduce the Taylor dispersion experiment at the microscale. Although preliminary experimental results are encouraging, there are a few items that can be improved further. Due to the fluctuation in the lighting of the laboratory room, particular attention needs to be placed on camera settings and calibration. One possible way to minimize the fluctuations in the laboratory lighting, is to run

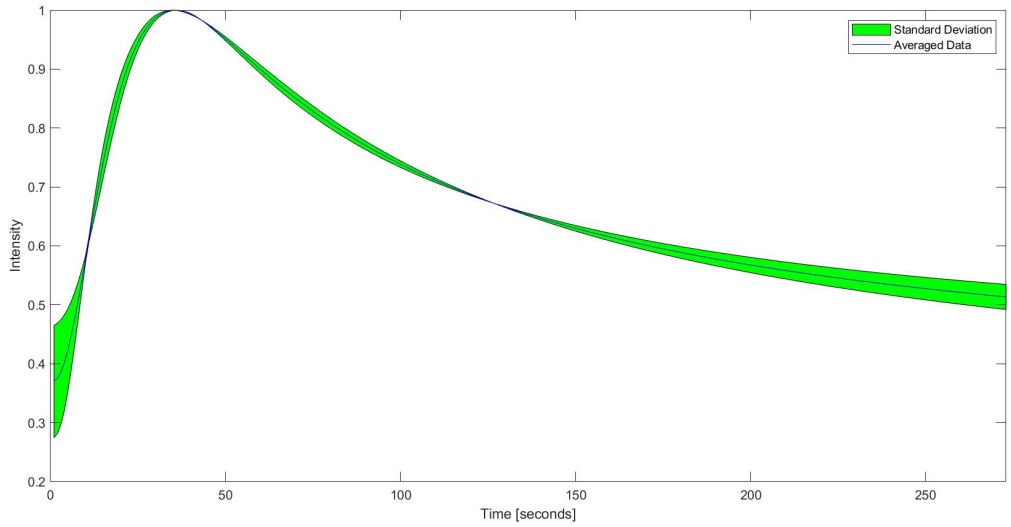

Figure 13: Plot of averaged data from two experimental runs (solid) with shading representing the standard deviation. Here, the curve shows how the dye intensity changes over time.

all experiments with the same parameters on a single day. Additionally, since the dye droplet is introduced manually for each experimental run, the experimental initial condition entering the channel is not always consistent trial to trial. One way to combat this is through the normalization of data, as shown in Section 4. Alternatively, a dye dropper could be purchased to inject the exact same small portion of dye for every experiment.

The next big step for this project is to focus on benchmarking the experimental dispersion coefficient against theoretical results. This can be done by fitting a Gaussian curve to the experimental data and extracting the experimental dispersion coefficient numerically. Then, the same protocol needs to be tested on microchannels of different aspect ratios defined as:

$$\lambda = \frac{a}{b}. \tag{13}$$

The testing on varying aspect ratios is important to prove that the experimental setup and protocol we designed works for other channel geometries beyond the one currently in use. This expands the reach of the method beyond this direct application.

6 Broader Impacts

This project has many great potential impacts both in the academic research and through real-world applications. Considering the Mechanical Engineering Code of Ethics, this experiment was designed and imple-

mented taking into account safety and environmental impacts. By working on a small-scale fluid mechanics project using an accessible rapid-prototyping technique, I was able to cut manufacturing and equipment costs by focusing closely and carefully on what the project needs and reducing waste. In fact, the microchannels produced for the experiment can be reused and very small amounts of a non-toxic solute are utilized (fluorescein dye salt solution in DI water). To focus further on sustainability, there is the possibility of switching to using recycled or recyclable materials to produce microchannels; this would reduce the environmental impact even more.

This experimental design and protocol have many applications beyond Taylor dispersion. For example, the manufacturing technique used to produce microchips could be repurposed to produce accessibly made microchannels in the fields of Chemistry, Biology, Biomedical Engineering, and Material Science. These cost-effective microchannels can be taken in many research directions and could be used, for example, to investigate mixing and de-mixing of solutes, to determine absorption rates, and to choose flow rates for larger experiments.

With the goal of opening a wide range of uses for this experimental protocol, the setup was specifically designed for maximum accessibility, repeatability, and transparency. By cutting the cost of microchannel fabrication from thousands of dollars down to $350, this fabrication can be done almost anywhere where there is a desk and electricity. Also with the precision of the tools being used, the protocol for fabrication is extremely repeatable. Including details for the procedure and protocol in this report, I aim to allow other scientists and engineers to be able to reproduce my results and use these techniques for their work. Ultimately Overall, the greatest impact that this project has is due to its economic factor and accessibility. By making microchannel fabrication an accessible procedure, we are opening the door for more people to be able to run experiments in fluid mechanics. Although the current setup I am using has some higher cost items, such as the Harvard Syringe Pump and the Nikon D500 camera, these microchannels can be used for much more than just observing Taylor dispersion. I hope that in the future, microchannels made in this low-cost way will be able to keep the field of fluid mechanics ever expanding to all.

Appendices

A Appendix A: Materials List

Polyimide Tape Double-sided adhesive polyimide tape 1 In. Wide x 36 Yards Long

Acetate Sheets Clear DuraLar™ Polyester Film .004"/100um thickness, 25 sheets pack

Silhouette Cameo 4 Craft Cutter 12" Black

Blade for Cameo 4 AutoBlade (Type B)

Tweezers Curved Medium Point Tip, 4.75 in

Tweezers Long Straight Very Fine Tip, 5.5 in

Tweezers Straight Broad Strong Point, 6 in

X-Acto Knife X-Acto No 1 Precision Knife — Z-Series, Craft Knife, with Safety Cap, #11 Fine Point Blade, Easy-Change Blade System

3D Printed Gaskets

Superglue Starbond EM-150 Medium, Instant Premium CA (Cyanoacrylate Adhesive) - Super Glue (for Woodturning, Pen Turning, Hobby, Lapidary, Acrylic Nails) (2 Ounce)

Glue Accelerant Starbond CA Glue Accelerator - for nstant Drying of Super Glue (6 ounces)

1 mL Syringe Plastic Syringe Luer Lock Connection, 1 ml Capacity. Pack of 10

3 mL Syringe Plastic Syringe Luer Lock Connection, 3 ml Capacity. Pack of 10

0.5 mL Glass Syringe 500 µL, Model 750 LT SYR

27 gauge plastic syringe tip Stainless Steel Dispensing Needle with Luer Lock Connection 1/2" Needle Length, 27 Gauge. Pack of 50

30 gauge plastic syringe tip Stainless Steel Dispensing Needle with Luer Lock Connection 1/2" Needle Length, 30 Gauge. Pack of 50

27 gauge plastic 2 in. syringe tip Kel-F Hub Needle 27 gauge, 2 in, point style 3, 6 pack

Capillary Tubing Masterflex Transfer Tubing, Microbore PTFE 0.012"IDx0.03"OD, 100ft rol

Havard Syringe Pump PUMP 11 ELITE INFUSION/ WITHDRAWAL PROGRAMMABLE SINGLE SYRINGE

Nikon D500 Camera

Recharable Camera battery EN-EL15 EN EL15a Battery Rechargeable, LP Charger Compatible with Nikon D7500, D7200, D7100, D7000, D850, D750, D500, D810a, D810, D800e, D800, D610, D600 More

Marco Lens Mitakon Zhongyi 20 mm f/2 Super Marco for Nikon Mount DSLR Cameras

Camera Flash Nikon D500 Digital Camera Lighting LED-36X On-Camera LED Video Light - with a Pack of 4 AAA NiMH Rechargable Batteries - 1000mAh

Tripod Vanguard Alta Pro 263AP Aluminum-Alloy Tripod Kit with PH-32 3-Way, Pan-and-Tilt Head

Light Panel Kaiser Slimlite Plano 5000K Battery/AC Lightbox (16.9 x 12.2")

Remote Trigger Remote Shutter Release Compatible for Nikon, Wireless Shutter Release Timer Remote Control Pixel TW-283 DC0/DC2 Compatible for Nikon D5200 D5300 D7100 D850 D800 D750 D610

Kimwipes 280 wipes/box, six pack

Microruler Shinwa H-3412A 6" 150 mm Rigid English Metric Zero Glare Satin Chrome Stainless Steel E/M Machinist Engineer Ruler/Rule with Graduations in 1/64, 1/32, mm and .5 mm

Fluorescein Sodium Salt 100 G

DeIonized Water

B Appendix B: Calibration Test Code

First all of the calibration photos were individually ran through this code:

```
%% Select the file to process
clear
[FileName,PathName] = uigetfile({'*.JPG', '*.jpg'},'MultiSelect', 'on');
FileName = cellstr(FileName);
FullPath = strcat(PathName,FileName);
[p,q] = size(FileName);
```

```
[ImageOrder, OrderPath] = uigetfile({'*.txt', '*.TXT'});

% depending on the number of images processed at once, this part takes a while
for i=1:q
    FullPath_i = char(FullPath(i));
    RGBCh = imread(FullPath_i); % RGB Channel data
    BlueCh = RGBCh(:,:,3); % B Channel data only
    Inv_BlueCh = 255 - BlueCh; % Invert blue channel data
    Data(:,:,i) = Inv_BlueCh; % makes full data matrix
end
disp('Done')

%   Crop and Rotate the region to analyze
% I = imread(FullPath_i);
Aref=imread(FullPath_i); %Read reference image file
imshow(Aref); %Show reference image
I2 = imcrop(Aref); %Crop reference image for orientation correction
imshow(I2); %Show cropped image

BW = im2bw(I2, graythresh(I2));
[B,L] = bwboundaries(BW,'noholes');
imshow(label2rgb(L, @jet, [.5 .5 .5]))
hold on

% BW1 = imbinarize(I2, 0.05); %Threshold image
% BW2 = bwareaopen(BW1,500); %consider only regions with at least 500 px
% BW2= imfill(BW2,'holes'); %fill in any holes in regions
%
% [B,L,N,A] = bwboundaries(BW2); %get region boundaries

ecount=0;
```

```
eslope = [];
for k=1:length(B)  %sweep through all boundaries
    boundary = B{k};
    %figure, %imshow(BW); hold on;
    plot(boundary(:,2), boundary(:,1),'w','LineWidth',2); %plot boundary on image

    %waitforbuttonpress;

%       aa=get(gcf,'CurrentCharacter');

%       if aa == 'a' %'a'  %press 'a' if acceptable
          ecount=ecount+1;
          P = polyfit(boundary(:,2),boundary(:,1),1);
          eslope(ecount)=P(1);
%       end
end

% aa=get(gcf,'CurrentCharacter');
%
% if aa == 'a' %'a'  %press 'a' if acceptable
%       ecount=ecount+1;
%       P = polyfit(boundary(:,2),boundary(:,1),1);
%       eslope(ecount)=P(1);
% end

imslope=mean(eslope); %take the average slope of all acceptable regions
Aref2=imrotate(Aref,atand(imslope)); %rotate image by avg slope

close all; %close all open figures
[~,RECT] = imcrop(Aref2); % crop
%%
```

```
clear PlotInfo
clear conc
clear NewImag
PlotInfo = [];
counter = 0;
FPS = 1; %Frames per second
RecordStart = 50; %Start time of recording
x0 = 150;
%Make a matrix with 3 rows one with time one with intensity one with sd
%Plot the top two elements of the matrix
%Theorectical curve should also be plotted in the background of the plot
%make a video
for i = 1:q % q is number of images you re processing
    I2 = Data(:,:,i);
    I3=imcrop(I2,RECT);
    I3 = cast(I3, 'double');
%         for non-rectangular pores, convert all values not within
%         fluorescein intensity range to NaN
    for m = 1:size(I3,2)
        for n = 1:size(I3,1)
            % set the value below according to specific set up,
            % check using imshow and seeing which intensity values
            % correlate to the channel walls vs. the pore
            if I3(n,m) > 255
                I3(n,m) = nan;
            end
        end
    end
    % calculate the mean, ignoring all values that are nan
    Ave_I = nanmean(I3,1); % (I, direction averaging over)
    conc(:,i) = Ave_I;
    NewImag(:,i) = Ave_I;
```

```
    % calculate the standard deviation of the mean, ignoring nan values
    for   j = 1:size(Ave_I,2)
        stdd = nanstd(I3(:,j));
        stdDev_I(:,j) = stdd;
    end
    allStdDev(:,i) = stdDev_I;
    PlotInfo = [PlotInfo ; counter NewImag(i) stdd];
    counter = counter + 1;
end


%% Graphing Data
%  close all
 %Building Curve Fit
 K = 0;
 xo = .02; %m
 t = 0:1:3;
 U = 0.00116; %m/s
 %c = (1/sqrt(4*pi*K*t))*exp(((xo-U*t)^2)/(4*K*t));
 plot(PlotInfo(:,1),PlotInfo(:,2))
 hold on
 %plot(c)
 xlabel('Time (Seconds)')
 ylabel('Intensity')
 %%
% ave_conc = mean(conc);
% frame.start=1;
% frame.end=25;
% close all
% final_conc = ave_conc(1,frame.start:frame.end);
% datastart = (frame.start-1)/FPS + RecordStart; % [seconds]
```

```
% dataend = datastart + ((size(final_conc,2)-1)/FPS);
% time = linspace(datastart, dataend, frame.end-frame.start+1);
% hold on
% plot(time,final_conc)
% xlabel('Time [s]')
% ylabel('Intensity')
% grid on
% xlim([datastart,dataend])
% [~,expframemax] = max(final_conc);
% exptmax = time(expframemax)
%%% Normalize / Peak change
% maxI = max(final_conc);
% minI = min(final_conc);
% N = (final_conc - minI) * 100/(maxI-minI);
% tmax = 150;
% T = time + (tmax - exptmax);
%%% %%
% close all
% Normalize = (conc - minI) * 100/(maxI-minI);
% Vis = uint8(Normalize);
% imshow(Vis)
%
```

Ever time the code ran, the maximum, mean, and minimum intensity values were stored. Then they were adding into this code to allow for a plot with error bars to be formed:

```
%All of the x and y coordinates for the plot with all five layers. y is the
%avaerage intensity for each of the layers
x1l = [0 .1 .3 1 3];
y1l = [39.1131  58.8154 75.2169 196.1078        245.0079];
x2l = [0 .1 .3 1 3];
y2l = [42.1027  90.7418 118.7163        241.3983        249.1858];
x3l = [0 .1 .3 1 3];
y3l = [44.4877  107.0515        150.0454        246.1543        254.8565];
```

```
x4l = [0 .1 .3 1 3];
y4l = [39.2281  114.1394        191.7617        245.7489        254.9998];
x5l = [0 .1 .3 1 3];
y5l = [45.0077  132.3675        212.701 248.3184        254.9921];

%Error for all of the five layers
min1l = y1l - [35.8     55.5324 72.6111 193.8621        243.8448];
max1l = y1l - [43.0208  62.3519 77.7222 198.6092        246.2529];
min2l = y2l - [39.4444  87.2389 116.3415        240.2849        247.2933];
max2l = y2l - [44.3333  93.5222 121.8943        242.6075        251.24];
min3l = y3l - [42.197   105.0417        147.0882        244.9286        254.5833];
max3l = y3l - [46.7955  109.6667        152.0539        247.3413        254.9917];
min4l = y4l - [38.1014  111.5   190.9267        244.1944        254.9825];
max4l = y4l - [40.1594  116.7692        192.6267        247.6296        255];
min5l = y5l - [44.0813  129.2824        210.2255        246.54  254.25];
max5l = y5l - [45.7805  135.4676        214.7157        250.18  255];

%X and Y coor for the concentration*layers plot
xCxL = [0 0 0 0 0 .1 .2 .3 .3 .4 .5 .6 .9 1 1.2 1.5 2 3 3 4 5 6 9 12 15];
yCxL = [12.8547 14.3038 14.3228 14.9372 15.6207 44.0933 65.1697 72.6883 83.7559
    110.7552 134.9665 117.5025 162.4975 183.7475 185.3860 205.3168 228.3559
    246.1088 246.4858 248.8459 247.1728 250.6134 254.9201 255 255];

%Error for the concentration*layers plot
minCxL = yCxL - [11.9181 12.7111 13.3072 14.1313 15.0705 42.6481 62.7037 71.3529
    82.7692 109.6852 133.5303  116.2351 160.8901 182.4529 184.0679 204.0833 227.4755
    245.3269 245.7044 248.1581 246.4394 249.6954 254.6984 254.9940 255];
maxCxL = yCxL - [13.9802 17.7222 15.6340 16.0455 16.3141 45.5450 68.0062 74.0490
    84.5641 112.0802 136.8333 118.4673 163.6241 184.6341 186.6358 206.7431 229.1544
    246.6827 247.2987 249.8675 248.1616 251.6954 254.9960 255 255];

x = 0:2;
```

```
y = 154.67*x+27.067;
%Graph for Concentration vs. Intensity
figure(1)
errorbar(x1l,y1l,min1l,max1l)
hold on
errorbar(x2l,y2l,min2l,max2l)
errorbar(x3l,y3l,min3l,max3l)
errorbar(x4l,y4l,min4l,max4l)
errorbar(x5l,y5l,min5l,max5l)
xlabel('Concentrations (g/L)')
ylabel('Intensity')
legend({'1 Layer','2 Layer','3 Layer','4 Layer','5 Layer'},'Location','southeast')
hold off

%Graph for Concentration*Layers vs. Intensity
figure(2)
errorbar(xCxL,yCxL,minCxL,maxCxL)
hold on
plot(x,y,'r--')
xlabel('Layers * Concentrations (g/L)')
ylabel('Intensity')
hold off
```

C Appendix C: Microchannel Fabrication

1. Open Silhouttee Studio and open the file in which you want to use to cut.
2. Plug computer into the craft cutter using a USB and turn the craft cutter on.
3. Cut a piece of polyimide tape that is longer than the version shown on the file.
4. Attach the polyimide tape cutting to the cutting board with the sticky side up. Use tape on the ends and side to ensure that it stays in place. Also make sure that the orientation of the tape matches the file.

5. Insert the cutting sheet into the craft cutter.
6. Press the send to craft cutter on the laptop and watch the microchannel be cut.
7. After the channel has been cut, remove it from the cutting board.
8. Using precise tweezers first take off the circular portions of the microchannel. Then remove the channel to create a negative.
9. Load a file to cut inlet and exit holes into acetate sheet.
10. Cut a piece of acetate that is longer than needed based on the file and attach it to the cutting board in the same way as was done with the polyimide tape.
11. Insert the cutting board into the craft cutter and send the file to be cut.
12. Once the acetate sheet has been cut, remove it from the cutting board.
13. Using circular ended tweezers, poke out the excess acetate sheet that is in the inlet and exit holes.
13. Wipe down the acetate sheet with a glass wipe to remove all finger prints.
14. Line up the inlet and exit holes on the acetate sheet with those on the polyimide tape and seal the channel by pressing them together.
14. Allow the sealed channel one day to make sure that everything is fully attached.
15. While waiting for the channel to seal make gasket covers using polyimide tape. These are small circles of 3 mm outer diameter with an inner diameter of 1.3 mm which matches the inlet and outlet holes on the microchannel. Cut these in polyimide tape using the same steps as with the microchannel.
16. Once the microchannel has settled for a day, the 3D printed gasket can be attached. Start by placing the microchannel under a fume hood.
17. Using tweezers remove one gasket cover from the polyimide tape.
18. Place the gasket cover around the inlet hole on the acetate sheet.
19. Stick at 27 gauge syringe tip into the 3D printed gasket. Using the syringe tip for guidance, place the gasket on top of the inlet hole and gasket cover. Make sure that the syringe is able to enter the channel so that you know fluid will be able to flow in it later.
20. Use super glue and go around the outside of the gasket. Since the gasket cover lifts the gasket up from the acetate, the glue will be sucked under the gasket due to capillary action.

21. To make the super glue dry faster, use an accelerator. Spray two times on top of the glue.

22. After twenty minutes, the gasket will be securely attached to the microchannel and the microchannel can be used for experiments.

D Appendix D: Dye Inlet Cover Fabrication

The fabrication of the dye inlet cover is as follows:

1. Starting in the Silhouette Cameo Software, draw out circles with diameters of 4 mm. I made 12 of these in columns of 3. Then on the same sheet draw out circles with a diameter of 1.3 mm. Again I made 12 of these so I would have to same of each.

2. Attach a layer of polyimide tape to the craft cutter sheet. Insert the sheet into the craft cutter in the same way as is done with the microchannel.

3. Once the craft cutter sheet is secured into the Silhouette Cameo 4 craft cutter, press start. The machine will cut out all 24 circles for you.

4. Remove the sheet of polyimide tape from the craft cutter. And store it in a cabinet to avoid dust till it needs to be used for an experiment.

5. When it is time to run an experiment, grab the circles on the polyimide tape. Using tweezers remove one of the 1.3 mm diameter circles off of the sheet. Be very careful when you do this so that all of the stickiness stays intact.

6. Next place the 1.3 mm diamter circle at the center of one of the 4 mm dimater circles.

7. Use the tweezers to press down on the 1.3 mm diamter circle to ensure that it is fully stuck to the 4 mm circle.

8. Finally use the tweezer to take the 4 mm diamter circle with the 1.3 mm diamter circle off of the sheet. And it is ready to be used for experiments.

E Appendix E: Matlab Codes

First all of the experiments are run through this data set in order to find the average intesitys over time.

```
%% Select the file to process
clear; clc; close all;
[FileName,PathName] = uigetfile({'*.JPG', '*.jpg'},'MultiSelect', 'on');
FileName = cellstr(FileName);
FullPath = strcat(PathName,FileName) ;
[p,q] = size(FileName);

% depending on the number of images processed at once, this part takes a while
for i=1:q
    FullPath_i = char(FullPath(i));
    RGBCh = imread(FullPath_i); % RGB Channel data
    BlueCh = RGBCh(:,:,3); % B Channel data only
    Inv_BlueCh = 255 - BlueCh; % Invert blue channel data
    Data(:,:,i) = Inv_BlueCh; % makes full data matrix
    % use the following to track progress
    disp('Processing image #');
    disp(i);
%     imshow(Inv_BlueCh);
end
disp('Done')

%%  Crop the region to analyze
I = imread(FullPath_i);
imshow(I);

%Coordinates of top left side
[x1,y1] = getpts;
disp(x1)
disp(y1)
%Coordinates of top right side
[x2,y2] = getpts;
disp(x2)
```

```
disp(y2)
%Coordinates of bottom left side
[x3,y3] = getpts;
disp(x3)
disp(y3)
%Coordinates of bottom right side
[x4,y4] = getpts;
disp(x4)
disp(y4)

c1 = sqrt(((x1(1)-x2(1)).^2)+((y2(1)-y1(1)).^2));
c2 = sqrt(((x3(1)-x4(1)).^2)+((y4(1)-y3(1)).^2));
a1 = abs(x1(1)-x2(1));
a2 = abs(x3(1)-x4(1));

theta1 = acosd(a1/c1);
theta2 = acosd(a2/c2);
imslope = (theta1 + theta2)/2;

I=imrotate(I,imslope); %rotate image by avg slope

close all; %close all open figures
[~,RECT] = imcrop(I); % crop

%% Data Analysis
close all
clear NewImag
t0=6;
tf =5;
for i = 1:q % q is number of images you re processing
    I = Data(:,:,i);
    I=imcrop(I,RECT);
```

```
    I = cast(I, 'double');
%         for non-rectangular pores, convert all values not within
%         fluorescein intensity range to NaN
    for m = 1:size(I,2)
        for n = 1:size(I,1)
            % set the value below according to specific set up,
            % check using imshow and seeing which intensity values
            % correlate to the channel walls vs. the pore
            if I(n,m) > 255 %change to calibration from intensity
                I(n,m) = nan;
            end
        end
    end
    % calculate the mean, ignoring all values that are nan
    Ave_I = nanmean(I,1); % (I, direction averaging over)
    NewImag(:,i)=Ave_I;
    tf= tf+1;
    % calculate the standard deviation of the mean, ignoring nan values
    for  j = 1:size(Ave_I,2)
        stdd = nanstd(I(:,j));
        stdDev_I(:,j) = stdd;
    end
    allStdDev(:,i) = stdDev_I;
    Max(i) = max(max(NewImag));
    Mean(i) = mean(NewImag, 'all');
    Min(i) = min(min(NewImag));
    ave_conc(i) = Mean(i);
end
% tspan = tf-t0+1;
% T = linspace(t0,tspan,tf);
T = t0:1:tf;
max_ave = max(ave_conc);
```

```
% ave_conc = ave_conc./max_ave;
%% Graphing Data
close all
hold on
plot(ave_conc)
grid on
xlabel('Frame')
ylabel('Averaged intensity of selected region')
%% Concentration over Time, calculation and plot
frameStart=1;
frameEnd=q;
FPS =1;
close all

final_conc = ave_conc(1,frameStart:frameEnd);

%% Graphing Data
close all
scatter(t0:1:tf,Mean)
hold on
xlabel('Time (Seconds)')
ylabel('Intensity')
```

Next all of the data is taking into this script to plot out the averaged experiments with one another:

```
clear; clc;
%Import all of your stored data
load('Consolidated18_2.mat');
load('Consolidated17.mat');
load('Consolidated14_2.mat');
load('Consolidated13_2.mat');

new = transpose(new);
newMax = max(max(new));
```

```
new = new./newMax;

new1 = transpose(new1);
newMax1 = max(max(new1));
new1 = new1./newMax1;

new2 = transpose(new2);
newMax2 = max(max(new2));
new2 = new2./newMax2;

new3 = transpose(new3);
newMax3 = max(max(new3));
new3 = new3./newMax3;

%Merging all data together
fullData = [new; new1; new2; new3];
maxData = max(fullData);
minData = min(fullData);
meanData = mean(fullData);

%Merging sets of data together
fullData2 = [new2; new1];
maxData2 = max(fullData2);
minData2 = min(fullData2);
meanData2 = mean(fullData2);

fullData3 = [new; new3];
maxData3 = max(fullData3);
minData3 = min(fullData3);
meanData3 = mean(fullData3);

T = 1:1:273;
```

```
figure(1)
errorbar(T,meanData,minData-meanData,maxData-meanData)
hold on
xlabel('Time [seconds]')
ylabel('Intensity')
hold off

figure(2)
plot(T,new);
hold on
plot(T,new1)
plot(T,new2)
plot(T,new3)
xlabel('Time [seconds]')
ylabel('Intensity')
legend('Experiment 1','Experiment 2','Experiment 3','Experiment 4')
hold off

figure(3)
plot(T,meanData);
hold on
xlabel('Time [seconds]')
ylabel('Intensity')
hold off

figure(4)
plot(T,new2);
hold on
plot(T,new1)
xlabel('Time [seconds]')
ylabel('Intensity')
```

```
legend('Experiment 1','Experiment 2')
hold off

figure(5)
scatter(T,new);
hold on
scatter(T,new3)
xlabel('Time [seconds]')
ylabel('Intensity')
legend('Experiment 1','Experiment 2')
hold off

figure(6)
errorbar(T,meanData3,minData3-meanData3,maxData3-meanData3)
hold on
xlabel('Time [seconds]')
ylabel('Intensity')
hold off

figure(7) %https://www.mathworks.com/matlabcentral/answers/494515-plot-standard-deviation-
T2 = [T, fliplr(T)];
inBetween = [minData3, fliplr(maxData3)];
fill(T2, inBetween, 'g');
hold on
plot(T, meanData3, 'b', 'LineWidth', .5);
legend('Standard Deviation', 'Averaged Data');
ylabel('Intensity')
xlabel('Time [seconds]')
```

References

[1] G. I. Taylor, "Dispersion of soluble matter in solvent flowing slowly through a tube," *Proceedings of the Royal Society of London. Series A. Mathematical and Physical Sciences*, vol. 219, no. 1137, pp. 186–203, 1953.

[2] I. Medina, "Determination of diffusion coefficients for supercritical fluids," *Journal of Chromatography A*, vol. 1250, pp. 124–140, 2012.

[3] D. Dutta, A. Ramachandran, and D. T. Leighton, "Effect of channel geometry on solute dispersion in pressure-driven microfluidic systems," *Microfluidics and Nanofluidics*, vol. 2, pp. 275–290, 2006.

[4] A. W. Taylor, "An accessible platform for numerical and experimental investigations of taylor dispersion," Master's thesis, Brown University, Providence, RI, 2019.

[5] F. Bernardi, *Space/Time Evolution in the Passive Tracer Problem*. PhD thesis, The University of North Carolina at Chapel Hill, 2018.

[6] G. I. Taylor, "Electrically driven jets," *Proceedings of the Royal Society of London. A. Mathematical and Physical Sciences*, vol. 313, no. 1515, pp. 453–475, 1969.

[7] "Laminar flow and turbulent flow."

[8] R. Aris, "On the dispersion of a solute in a fluid flowing through a tube," *Proceedings of the Royal Society of London. Series A. Mathematical and Physical Sciences*, vol. 235, no. 1200, pp. 67–77, 1956.

[9] A. W. Taylor and D. M. Harris, "Optimized commercial desktop cutter technique for rapid-prototyping of microfluidic devices and application to taylor dispersion," *Review of Scientific Instruments*, vol. 90, no. 11, p. 116102, 2019.

[10] S. M. Scott and Z. Ali, "Fabrication methods for microfluidic devices: An overview," *Micromachines*, vol. 12, no. 3, p. 319, 2021.

[11] H.-T. Nguyen, H. Thach, E. Roy, K. Huynh, and C. M.-T. Perrault, "Low-cost, accessible fabrication methods for microfluidics research in low-resource settings," *Micromachines*, vol. 9, no. 9, p. 461, 2018.

[12] G. Lee, "Dispersion control in deformable microchannels," Master's thesis, Brown University, Providence, RI, 2020.

[13] "Silhouette cameo design software." https://www.silhouetteamerica.com/featured-product/cameo. Accessed: 2023-03-28.

[14] M. Aminian, F. Bernardi, R. Camassa, D. M. Harris, and R. M. McLaughlin, "How boundaries shape chemical delivery in microfluidics," *Science*, vol. 354, no. 6317, pp. 1252–1256, 2016.